Na et al., http://www.jcb.org/cgi/content/full/jcb.201407130/DC1

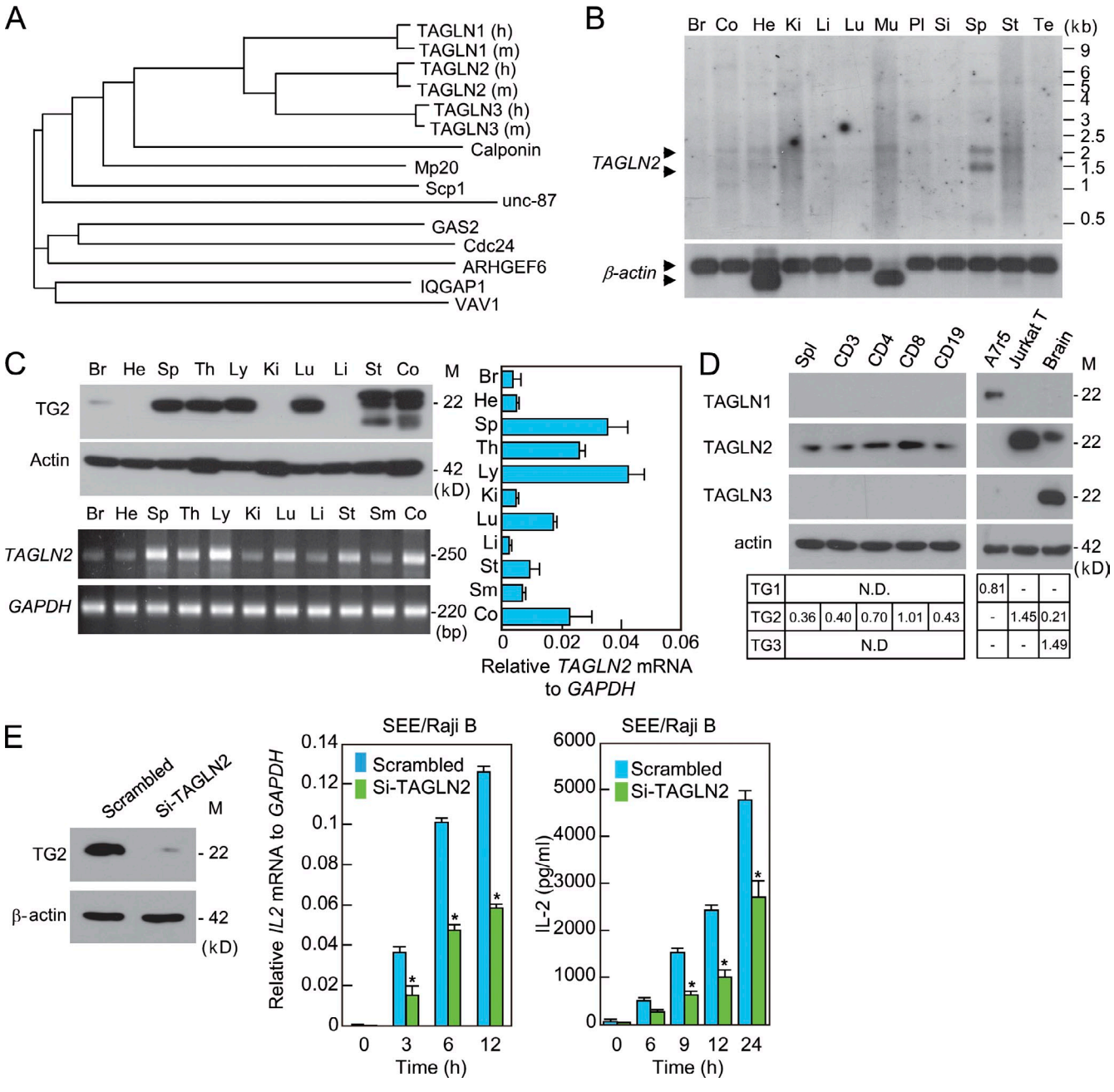

Figure S1. **TAGLN2 is expressed in immunogenic tissues and cells, and TAGLN2 knockdown reduces T cell activation.** (A) The phylogenetic tree of TAGLN2 deduced by ClustalW software. The tree shows the evolutionary relationships among single CH domain-containing proteins. (B and C) Tissue distribution of TAGLN2 in humans (h) and mice (m). (B) Northern blot analysis in human tissues. *TAGLN2* is indicated by arrowheads located at 1.4 and 1.6 kb. Human β-actin served as a loading control. (C) A Western blot (top left), RT-PCR (bottom left), and real-time qPCR (right) analysis of TAGLN2 (TG2) in mouse tissues. M, molecular mass; Br, brain; He, heart; Li, liver; Lu, lung; St, stomach; Co, colon; Ki, kidney; Mu, muscle; Sp, spleen; Th, thymus; Ly, lymph node; Si, small intestine; Pl, placenta; Te, testis. (D) Western blot analysis of TAGLN1, TAGLN2, and TAGLN3 in splenocytes (spl), T cell subsets (CD3, CD4, and CD8), and a B cell subset (CD19) purified from mice. TAGLN2 expression was determined using a Western blot. A7r5 cells and brain were used as positive controls for TAGLN1 and TAGLN3. Protein band intensities were quantified using ImageJ. Protein intensities of each sample quantified using ImageJ were normalized by intensity of actin (bottom). All data shown are representative of three independent experiments. (E) Human PBLs were transfected with either scrambled siRNA (70 nM) or siRNA targeting *TAGLN2*. After 48 h, the expression of *TAGLN2* was determined using a Western blot (left), and the cells were incubated with SEE-pulsed Raji B cells. *IL2* mRNA and IL-2 secretion was assessed using real-time qPCR and ELISA. *, $P < 0.05$ compared with scrambled siRNA-treated cells. Error bars are means ± SD.

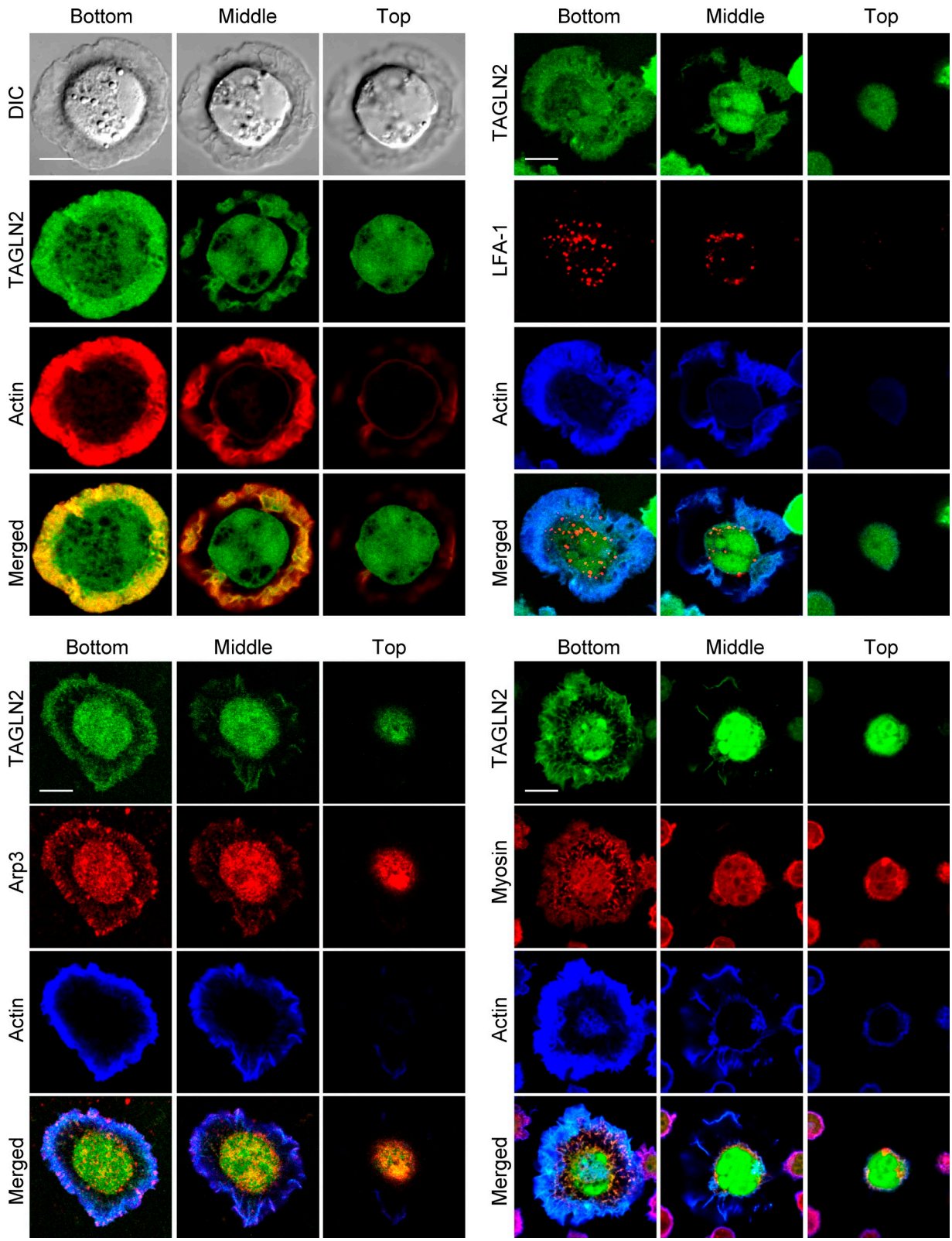

Figure S2. **Localization of TG2, actin, LFA-1, Arp3, and myosinII.** Images are individual z stacks acquired as optical sections from bottom to top. Merged z-stack images are shown in Videos 2–4. DIC, differential interference contrast. Bars, 10 µm.

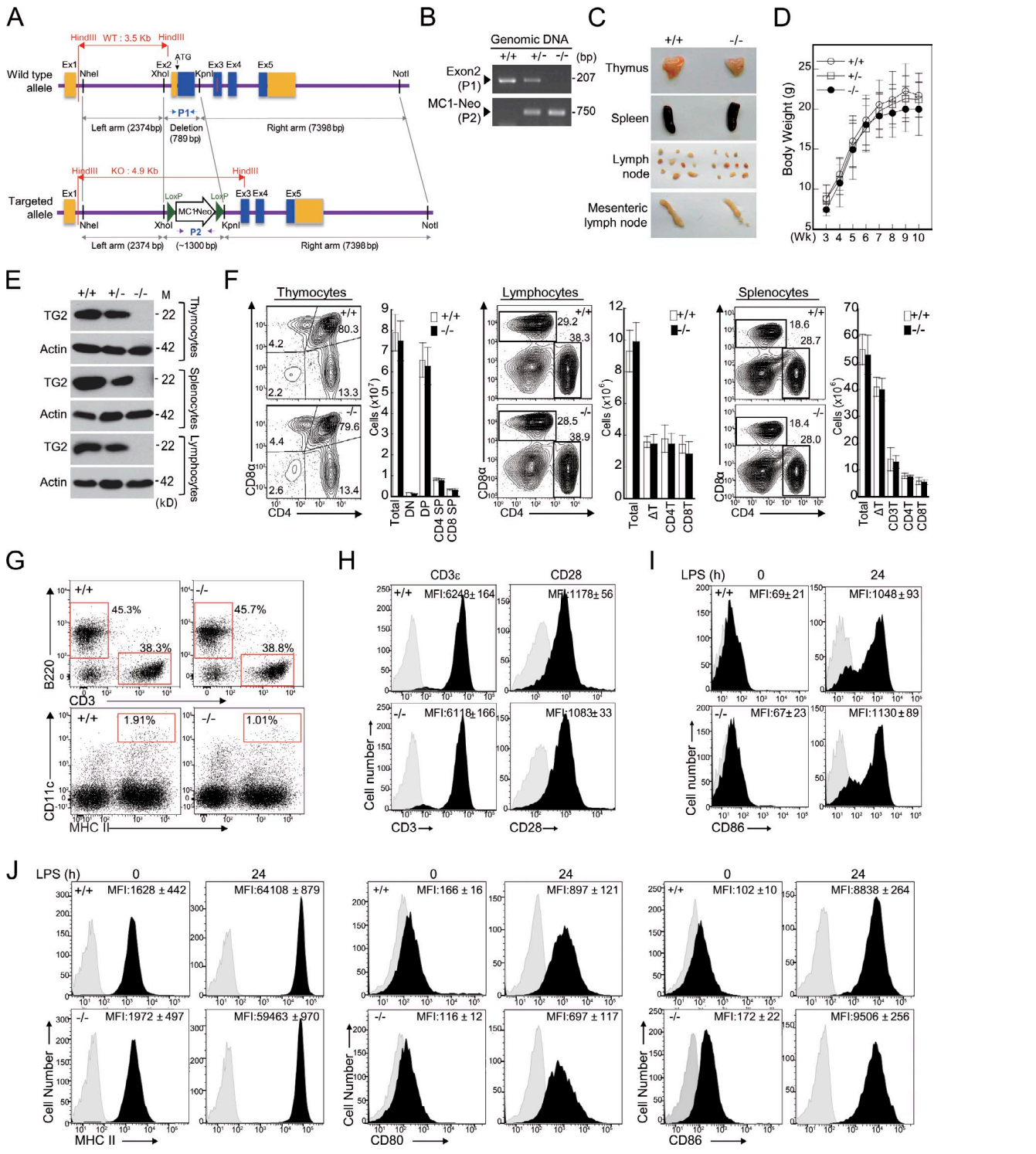

Figure S3. **Generation of *TAGLN2* knockout mice and flow cytometric analysis.** (A) Schematic representation of the targeting strategy used to delete the *TAGLN2* gene. The WT allele and the targeted mutant allele generated by homologous recombination are depicted. P1 (a primer set for the exon 2 of *TAGLN2* deleted after homologous recombination) and P2 (a primer set for the MC1-neomycin [neo] cassette replaced by homologous recombination) were used for genotyping. Ex, exon. (B) PCR genotyping. Genomic DNA was extracted form mouse ear tissue. The WT (+/+) and heterozygote mutant (+/−) alleles were detected with P1, but the homozygote (−/−) alleles were not detected with this primer. Using the P2 primer set, the heterozygote and homozygote alleles, but not the WT allele, were detected. (C and D) Phenotype comparison of $TAGLN2^{+/+}$ and $TAGLN2^{-/-}$ mice. (C) Photomeasurement of the immunogenic organs from $TAGLN2^{-/-}$ mice. (D) Body weight measurement for 10 wk. The data represent the means ± SD (n = 10). (E) Expression of TAGLN2 protein in thymocytes, splenocytes, and lymphocytes obtained from $TAGLN2^{+/+}$ and $TAGLN2^{-/-}$ mice was determined by Western blot analysis. Results are representative of two independent experiments. M, molecular mass. (F) Thymocytes, lymphocytes, and splenocytes from $TAGLN2^{-/-}$ mice were tested for the presence of $CD4^+$ and $CD8^+$ cells. The percentage of cells in each quadrant or box is indicated. Mean cell numbers of subsets are shown in the bar graph. (G) Populations of T cells ($CD3^+CD19^-$), B cells ($CD3^-CD19^+$), and DCs ($MHCII^+CD11c^+$) in splenocytes were determined using flow cytometry. Dots represented each population were shown within red boxed area. (H) CD3-ε and CD28 expression on $CD3^+$ T cells isolated from $TAGLN2^{+/+}$ and $TAGLN2^{-/-}$ mice were determined using flow cytometry (black shading). MFI, mean fluorescence intensity. (I and J) $CD11c^+$ splenic DCs (I) and $CD19^+$ splenic B cells (J) were activated by 1 μg/ml lipopolysaccharide for 24 h, and then, CD86, MHCII, and CD80 expression was determined using flow cytometry (black shading). Data are representative of three separate experiments. Gray shading shows isotype control.

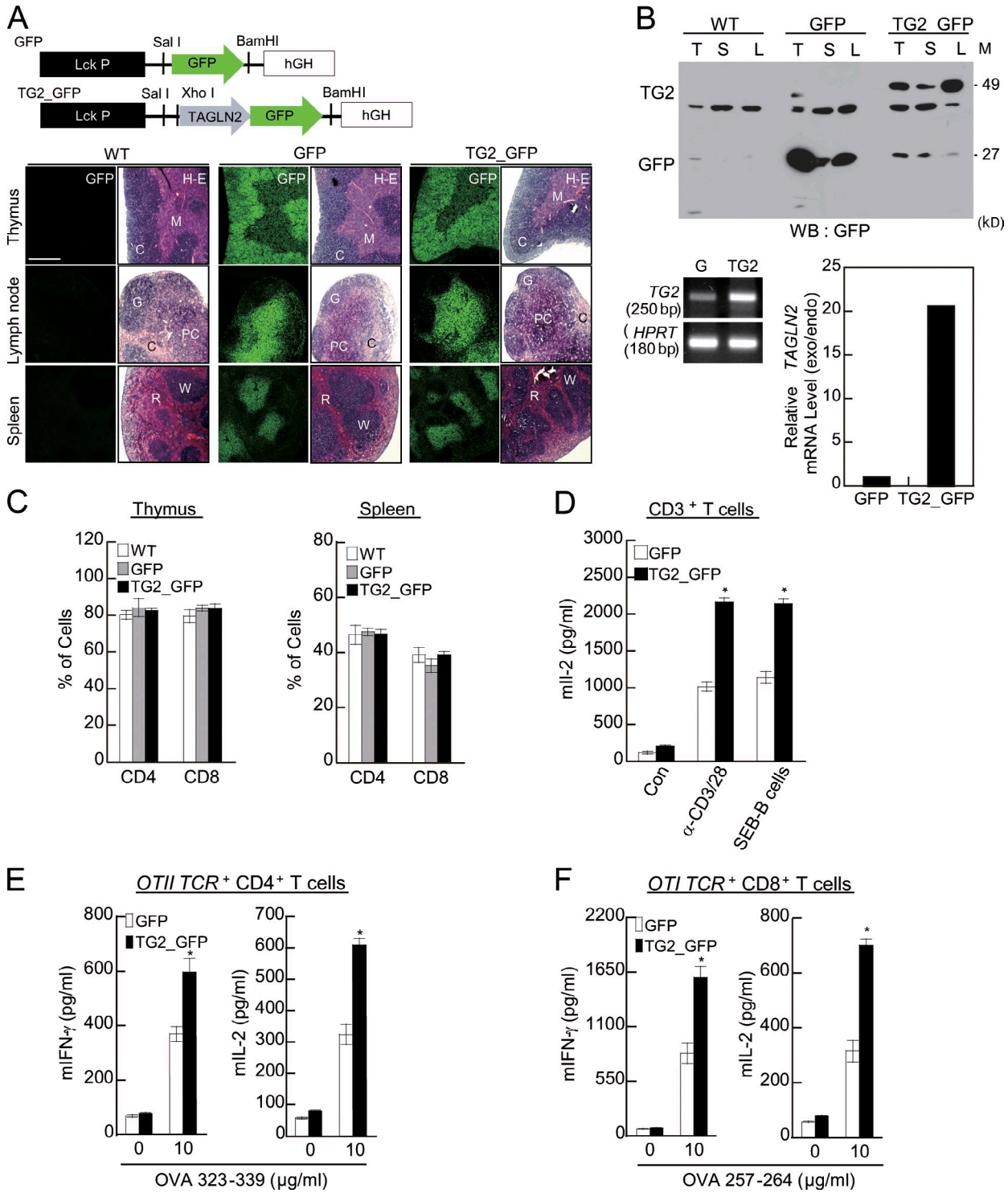

Figure S4. **Generation of GFP-T or TAGLN2 (TG2)_GFP-T transgenic mice and analysis of T cell activation in response to TCR stimulation.** (A) Vector construction for establishing GFP-T or TG2_GFP-T transgenic mice. For ectopic expression of each gene in T cells, the *Lck* promoter (Lck P) was used. (top) *GFP* or *TG2_GFP* was inserted between *Lck* P and the human growth hormone gene (hGH). (bottom) Tissue sections were imaged by confocal microscopy to determine GFP and TG2_GFP expression in various lymphoid tissues, including the thymus, spleen, and lymph node. Hematoxylin and eosin (H-E) staining served as a control. Data are representative of two independent experiments. C, cortex; M, medullar; G, germinal center; PC, paracortex; R, red pulp; W, white pulp. Bar, 100 μm. (B, top) Expression of GFP or TG2_GFP in lymphoid tissues including the thymus (T), spleen (S), and lymph node (L) was determined by Western (WB) blot analysis. The level of exogenous *TAGLN2* mRNA in splenic T cells of transgenic mice was assessed by RT-PCR (bottom left) and real-time PCR (bottom right). Data are representative of three experiments. G, GFP; exo, exogenous; endo, endogenous; M, molecular mass. (C) Thymocytes and splenocytes were stained with either a PerCP-Cy5.5–conjugated anti-CD4 or a PerCP-Cy5.5–conjugated anti-CD8 antibody, and then, cells were analyzed by flow cytometry. The mean number of CD4 and CD8 cell subsets is shown in the bar graph. The results are the means ± SD of triplicate experiments. (D) $CD4^+$ or $CD8^+$ T cells were purified from GFP-T or TG2_GFP-T transgenic mice. Cells were then stimulated with an anti-CD3/28 or incubated with SEB-pulsed $CD19^+$ B cells for 24 h, and the level of IL-2 cytokine production was measured by ELISA. The results are the means ± SD of triplicate experiments. *, $P < 0.05$ compared with GFP-T cells. Con, control. (E and F) *OTII* TCR^+ $CD4^+$ (E) or *OTI* TCR^+ $CD8^+$ (F) T cells from GFP-T and TG2_GFP-T transgenic mice were stimulated with or without OVA-loaded DCs for 24 h. IFN-γ and IL-2 in the supernatant were measured by ELISA. *, $P < 0.05$ compared with GFP-T cells. The results are means ± SD of triplicate experiments.

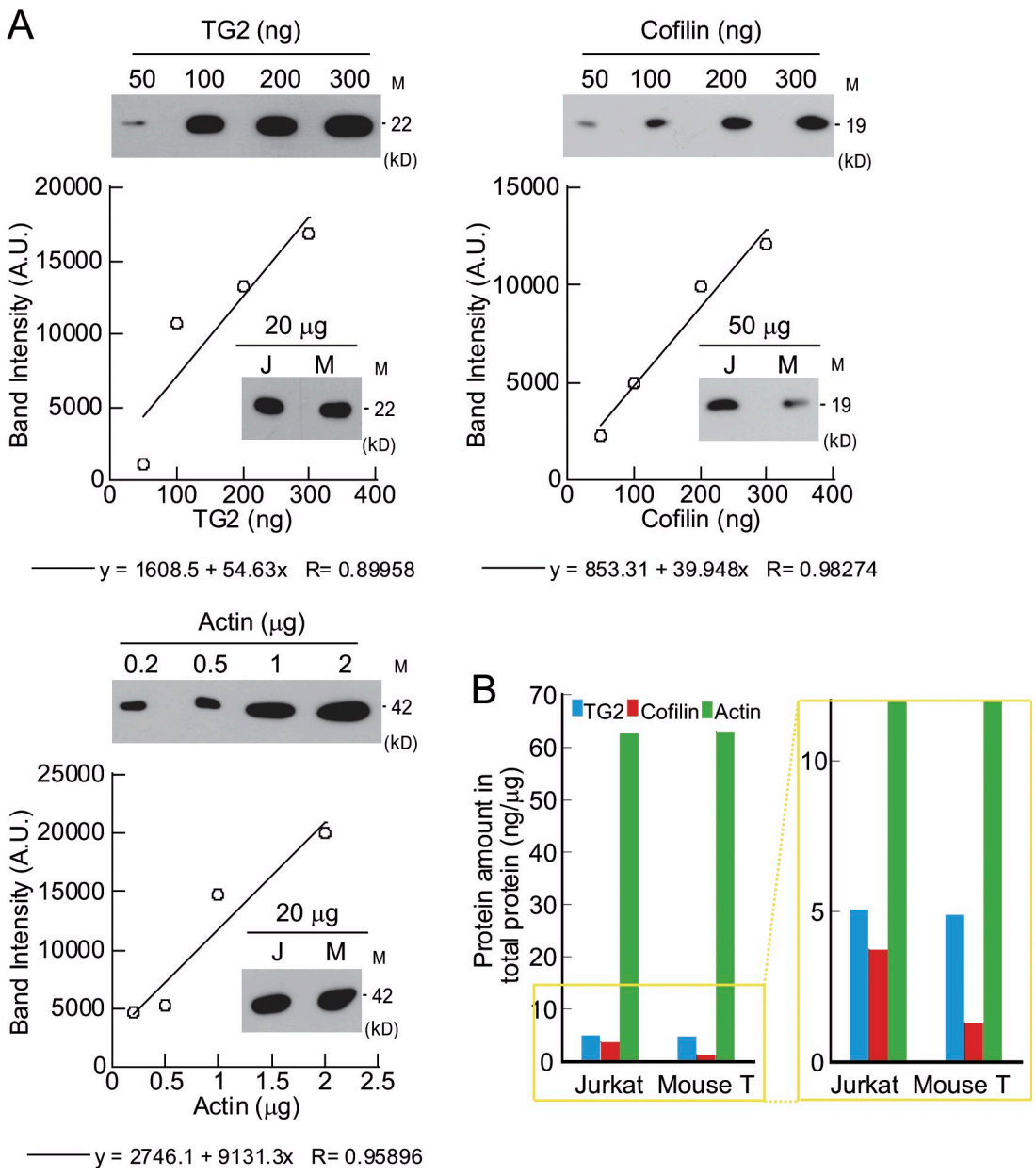

Figure S5. **Cellular concentrations of TAGLN2, cofilin, and actin.** Quantitative Western blot analysis was performed to measure the amount of each protein in T cells. (A) To generate a standard curve, recombinant TAGLN2, cofilin, and actin proteins of known concentrations were detected by Western blotting, and band intensities were quantified using densitometry on developed films. Total lysates of Jurkat T cells (J) and mouse T cells (M) were loaded into wells, and were blotted with antibodies against each protein. Band intensities were also measured by densitometry. (B) Protein amounts, per 1 μg of total cell lysate, were calculated by comparison of band intensities to the standard curve and then divided by the amount of total cell lysate loaded. The boxed area (yellow) is represented as the zoomed portion of graph in the right panels. All data shown are representative of three independent experiments. A.U., arbitrary unit; M, molecular mass.

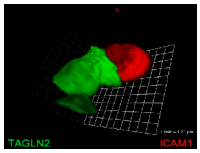

Video 1. **Three-dimensional view of TAGLN2_GFP and ICAM-1 localization at the contact site of T–B cells.** J-TG2_GFP cells were conjugated with SEE-loaded Raji B cells, which were stained for ICAM-1 with cy5-conjugated CBRIC1/11 (red). Z-stack images were taken by a laser scanning confocal microscope (FV1000; Olympus). 3D image reconstruction and localization analysis were performed using Volocity software (PerkinElmer). This video corresponds to Fig. 1 E.

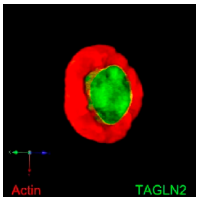

Video 2. **Localization of TAGLN2 and F-actin in Jurkat T cells placed on anti-CD3/28–coated coverslips.** J-TG2_GFP cells on anti-CD3/28 coverslips were stained for F-actin with TRITC-phalloidin (red). Z-stack images were obtained using a laser scanning confocal microscope (FV1000; Olympus). 3D image reconstruction and localization analysis were performed using Volocity software (PerkinElmer). This video corresponds to Fig. 1 F.

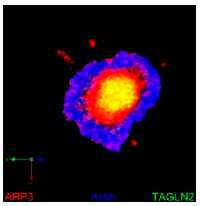

Video 3. **Localization of TAGLN2, Arp3, and F-actin in Jurkat T cells placed on anti-CD3/28–coated coverslips.** J-TG2_GFP cells on anti-CD3/28 coverslips were stained for Arp3 with anti-Arp3 antibody and TRITC-conjugated anti–mouse IgG (red) and F-actin with Alexa Fluor 647–phalloidin (blue). Z-stack images were obtained using a laser scanning confocal microscope (FV1000; Olympus). 3D image reconstruction and localization analysis were performed using Volocity software (PerkinElmer). This video corresponds to Fig. 1 F.

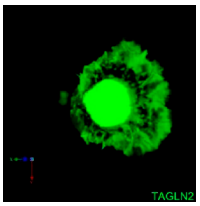

Video 4. **Localization of TAGLN2, myosin IIA, and F-actin in Jurkat T cells placed on anti-CD3/28-coated coverslips.** J-TG2_GFP cells on anti-CD3/28 coverslips were stained for myosin IIA with anti–myosin IIA antibody and TRITC-conjugated anti–mouse IgG (red) and F-actin with Alexa Fluor 647–phalloidin (blue). Z-stack images were obtained using a laser scanning confocal microscope (FV1000; Olympus). 3D image reconstruction and localization analysis were performed using Volocity software (PerkinElmer). This video corresponds to Fig. 1 F.

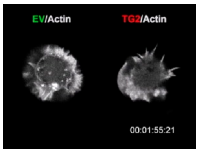

Video 5. **Real-time F-actin ring formation during J-GFP or J-TG2_GFP cell spreading on anti-CD3/28–coated coverslips.** J-GFP (empty vector [EV]) and J-TG2_GFP (TG2) cells were transfected with LifeAct_mCherry (white) and loaded on anti-CD3/28 coverslips. Time-lapse images at the bottom site were acquired by a laser scanning confocal microscope (FV1000; Olympus). Frames were taken every 20 s for 1,000 s. Videos are displayed at a rate of 3.4 frames/s. The timestamp is given hours, minutes, seconds, and milliseconds. This video corresponds to Fig. 2 A.

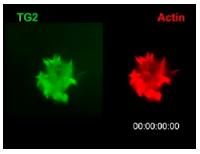

Video 6. **Dynamic localization of TAGLN2 and actin during J-TG2_GFP cell spreading on anti-CD3/28–coated coverslips.** J-TG2_GFP cells were transfected with LifeAct_mCherry (red), and loaded on anti-CD3/28 coverslips. Time-lapse images at the bottom site were acquired by a laser scanning confocal microscope (FV1000; Olympus). Frames were taken every 20 s for 1,000 s. Videos are displayed at a rate of 3.4 frames/s. The timestamp is given hours, minutes, seconds, and milliseconds. This video corresponds to Fig. 2 A.

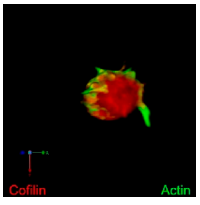

Video 7. **Localization of cofilin and F-actin in Jurkat T cells placed on anti-CD3/28–coated coverslips.** J-TG2_GFP cells were transfected with cofilin/S3A_pERFP_N1 and placed on anti-CD3/28 coverslips. Cells were stained for F-actin with Alexa Fluor 647–phalloidin (blue). Z-stack images were obtained using a laser scanning confocal microscope (FV1000; Olympus). 3D image reconstruction and localization analysis were performed using Volocity software (PerkinElmer). This video corresponds to Fig. 8 B.

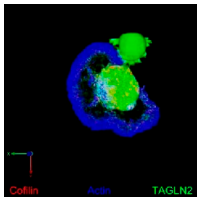

Video 8. **Localization of cofilin, TAGLN2, and F-actin in Jurkat T cells placed on anti-CD3/28–coated coverslips.** Jurkat T cells were transfected with cofilin/S3A_pERFP_N1 and placed on anti-CD3/28 coverslips. Cells were stained for F-actin with Alexa Fluor 647–phalloidin (green). Z-stack images were obtained using a laser scanning confocal microscope (FV1000; Olympus). 3D image reconstruction and localization analysis were performed using Volocity software (PerkinElmer). This video corresponds to Fig. 8 B.